A&A 378, 455–465 (2001)
DOI: 10.1051/0004-6361:20011210

Astronomy & Astrophysics

K 413, a star near the AGB in the globular cluster M 12

V. G. Klochkova[1,2] and N. N. Samus[3,4]

[1] Special Astrophysical Observatory, N. Arkhyz 369167, Russia
[2] Isaac Newton Institute of Chile, SAO Branch, Russia
[3] Institute of Astronomy of Russian Acad. Sci., 48, Pyatnitskaya Str., Moscow 109017, Russia and Sternberg Astronomical Institute of Moscow University, 13, University Ave., Moscow 119899, Russia
[4] Isaac Newton Institute of Chile, Moscow Branch, Russia

Received 27 June 2001 / Accepted 20 August 2001

Abstract. CCD spectra obtained with the echelle spectrometer of the 6-meter telescope were used to determine, by the model atmospheres method, the fundamental parameters ($T_{\rm eff} = 4800$ K, $\log g = 0.7$) and detailed chemical abundances for the star K 413, a member of the globular cluster M 12. The resulting value, [Fe/H] $= -1.38$, is the first metallicity determination for M 12 using high-resolution spectra. The main characteristic feature of the star's atmospheric chemical abundance pattern is a large oxygen excess, [O/Fe] $\approx +2$. The *s*-process elements are probably slightly depleted compared to metallicity: [X/Fe] $= -0.04$ for yttrium and zirconium, [Ba/Fe] $= -0.12$ for barium. Abundances of the heavier elements: La, Ce, Nd, and Pr, do not differ, relative to iron, from the solar ones: [heavy/Fe] $= 0.0$. The europium excess, [Eu/Fe] $= +0.48$, is typical of members of low-metallicity globular clusters. The spectrum of K 413 shows, for the Hα line, an variable absorption and emission profile. From its high luminosity and chemical abundance anomalies, we can suppose that K 413 is in an evolutionary stage after the AGB. In the spectrum, we find absorption details that can be identified with diffuse interstellar bands displaced by 16 km s^{-1} to longer wavelengths relative to the star's velocity.

Key words. globular clusters: general – globular clusters: individual M 12 – stars: abundances – stars: atmospheres – stars: AGB and post-AGB

1. Introduction

This paper continues the series of our publications on the studies of stars at a short-lived evolutionary stage of the transition from the asymptotic giant branch (AGB) to planetary nebulae (cf. Klochkova et al. 2000 and references therein). The main goal of this program is to investigate anomalies of the chemical composition for the objects that have experienced a sequence of changes of their energy sources, mixing, and matter dredge-up from layers with modified chemical composition to the surface.

Stars at late stages of evolution, members of globular clusters, are of particular interest: their cluster membership makes their evolutionary stage and luminosity known more confidently than for stars in the galactic field. Simultaneously, globular cluster membership makes high spectral resolution observations of a star difficult because such clusters are very distant from the Sun. Besides, it is difficult to prove membership, especially for stars above the horizontal branch. In fact, only one of the generally-used criteria, the value of the radial velocity, is decisive for such objects. For this reason, accurate radial velocity measurement is a special task.

Send offprint requests to: V. G. Klochkova,
e-mail: valenta@sao.ru

In this paper, we present the results of our spectroscopic study of a faint star ($V = 12\overset{\rm m}{.}83$), K 413 (the number according to Küstner 1933), in the globular cluster M 12. In Racine (1971), the star has the number II-02-51; Zinn et al. (1972) list it as No. 8. Note that Zinn et al. (1972) compiled a large list of globular-cluster stars above horizontal branches in the color–magnitude diagrams and suggested to call them "UV-bright stars". The Harris (1996) catalog contains the following principal characteristics of this cluster: the mean radial velocity, $V_{\rm r} = -42.2$ km s^{-1} (relative to the local standard of rest, $V_{\rm lsr} = -26.4$ km s^{-1}); the mean color excess, $E(B-V) = 0.19$; the distance modulus, $m - M = 14\overset{\rm m}{.}02$; the distance, $d = 4.9$ kpc. The cluster's modern $V-(B-V)$ diagram can be found in Brocato et al. (1996). The diagram shows that K 413 is brighter than AGB stars with the same $(B-V)$ color index by one magnitude, so it can be considered as a post-AGB star. The high probability of the cluster membership for K 413 follows from proper motions of stars in the field of the cluster M 12 (Geffert et al. 1991) as well as from radial velocity data. From moderate-resolution spectra, Harris et al. (1983) measured radial velocities for a sample of such stars and were able to confirm membership of several UV-bright stars in the globular clusters M 12 and M 56 (in

particular, the membership of K 413 in M 12). The latter authors give the mean velocity value $V_r = -41.3\,\mathrm{km\,s^{-1}}$ for stars in the cluster M 12. For K 413, they derived the velocity $V_r = -44.2\,\mathrm{km\,s^{-1}}$.

Our paper is the first presentation of results based upon high-resolution spectra of objects in the cluster M 12. Section 2 briefly describes the techniques of observations, reductions, and analysis. Section 3 presents the results of our determination of the detailed atmospheric chemical composition of K 413. Section 4 contains discussion and main conclusions.

2. Observations and data analysis

2.1. Observations and reductions of the spectra

Two echelle spectra in the 4300–7800 Å range were obtained in the prime focus of the 6 m telescope, with the echelle spectrometer PFES (Panchuk et al. 1998). The mean times of observations are collected in Table 1. PFES is equipped with a 1160×1040 pixel CCD, designed at the Special Astrophysical Observatory; the pixel size is $16 \times 16\,\mu$m. The spectrometer's resolution is up to 17 000 in a wide wavelength range. The spectrum of a Th–Ar lamp was recorded for wavelength calibration. Processing of the 2D images (standard procedures of dark current subtraction, removal of cosmic rays, subtraction of scattered light, extraction of echelle orders) made use of the ECHELLE context of the MIDAS system (version 1998). Spectrophotometric and positional measurements of 1D spectra used the DECH20 package (Klochkova & Galazutdinov 1991; Galazutdinov 1992). The signal-to-noise ratio of the spectral portions used for the chemical abundance analysis considerably exceeded 100, enabling us to measure equivalent widths of weak lines, to 10–15 mÅ. Note that results presented here are based mainly on the spectrum s27605, while the second spectrum s31208 was obtained and used for comparison only.

2.2. Determination of model parameters

To derive the basic parameters of the stellar model atmospheres: effective temperature, $T_{\rm eff}$, and surface gravity, $\log g$, for computations of chemical abundances and of synthetic spectra, we used the grid of model atmospheres computed by Gustafsson et al. (1975) in the hydrostatic approximation.

The wide spectral range simultaneously recorded by the PFES echelle spectrometer makes it possible to determine the principal model parameters, $T_{\rm eff}$ and $\log g$, using only spectroscopic criteria free of the influence of interstellar and circumstellar reddening.

The "photometric" criteria are used widely for temperature determination, especially for metal poor stars. But this method is not useful for the star K 413. For objects at an advanced evolutionary stage it is specially difficult to account for reddening. We do not know a priori normal (intrinsic) colours for such an object of uncertain evolution any stage and uncertain chemical composition. Using average "$T_{\rm eff}$–color" calibrations and average colour-excess, we do not take into account peculiarities of atmospheres of individual stars. This, in turn, may lead to essential errors in temperature and then to incorrect conclusions on chemical composition and evolution stage since the expected values alterations of abundances in evolution are small, they exceed possible systematic errors insignificantly. Therefore we determined the effective temperature by the traditional method, from the condition of independence of neutral iron abundance upon excitation potentials of the corresponding lines (Fig. 1a). The surface gravity was chosen from the ionization balance for neutral and ionized atoms of iron, and the microturbulent velocity from the condition of independence of iron abundance and line intensity (Fig. 1b).

When determining the model atmospheric parameters and calculating chemical composition, it is important to restrict the study to lines of low and moderate intensities, with equivalent widths $W \le 0.25$ Å, since the stationary plane-parallel atmosphere approximation can be inadequate for the presentation of the strongest spectral features. Besides, some of the strong absorptions can be distorted by the circumstellar envelope and, if the spectral resolution is not sufficient, the intensity of the envelope components will be included in the intensity of the components formed in the atmosphere.

The equivalent widths, oscillator strengths (gf) of the spectral lines used to determine the model parameters, and the computed abundances of elements are presented in Table "K413-LIN" available upon request by e-mail: `valenta@sao.ru`, and via ftp at the FTP-directory: `lnf1.sai.msu.ru/pub/PEOPLE/samus/K413-LIN` (or `ftp.sao.ru/pub2/sslab/K413-LIN`).

The effective temperature was thus determined from their dependence of the iron abundance on the excitation potential of the lower levels of the lines used. An additional criterion for the method's reliability is the absence of a similar dependence for other chemical elements, also represented in the spectra by numerous lines (for example, Si I, Ca I, Sc II, Ti I, Ti II, Cr I, Cr II, Ni I). Besides, in the case of reliable determination of the microturbulent velocity ξ_t, individual abundances are independent of the equivalent widths of the lines used in computations. The abundances of silicon, titanium, and chromium, determined from lines of neutral atoms as well as from lines of ions, agree within the uncertainties of the method. This evidence for the correctness of our determination of the atmospheric gravity comes from the ionization balance for atoms of iron. Generally, the self-consistency of the parameters shows that the homogeneous model atmospheres applied here are usable for computations of weak lines in the LTE approximation. The resulting parameters of the model atmospheres are, $T_{\rm eff} = 4800\,\mathrm{K}$, $\log g = 0.7$, $\xi_t = 3.5\,\mathrm{km\,s^{-1}}$.

The characteristic uncertainty of model parameter determinations, on average for a star with temperature

Table 1. Heliocentric radial velocities of K 413, measured from different details in its spectra. Numbers of lines used to derive the velocity value are indicated in brackets. V_r(em, blue) is the velocity measured from the blue-shifted emission peak; V_r(em, red) is the velocity measured from the red-shifted emission peak of H_α.

Spectrum	JD	$V_\odot$, km s^{-1}						
		Metals (n)	Hα			Na D1, D2		DIB (n)
			em, blue	abs	em, red	Stellar	Circumstellar	
s27605	2451708.378	−40.96 (453)	−88.2	−43.8	+17.4	−38.6 (2)	−24.6 (2)	−24.9 (8)
s31208	2452072.403	−41.48 (125)	−106.9	−53.4	+16.0	−40.9[1] (2)	−30.06[1] (2)	−23.58 (4)

[1] – This value was determined with a high uncertainty.

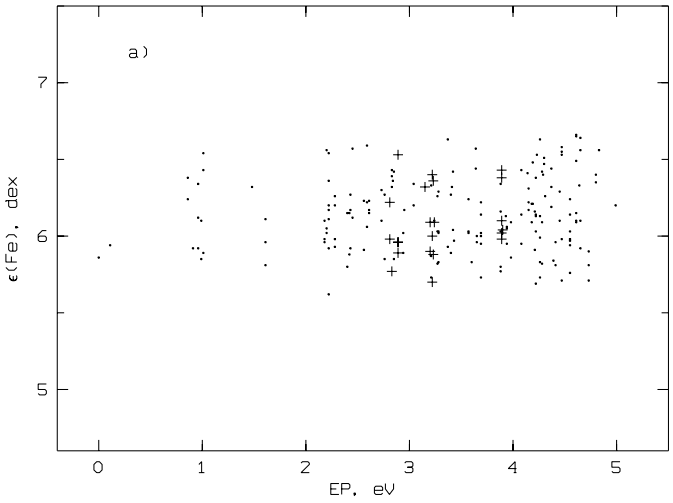

Fig. 1. a) Iron abundance FeI (circles) and FeII (crosses) calculated for K 413 with model parameters from Table 3 using lines with different excitation potencials EP of a low lewel.

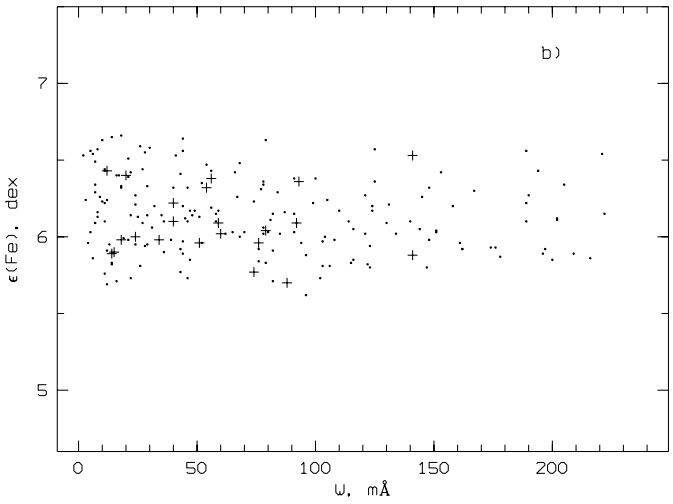

Fig. 1. b) The same as a function of the equivalent width W.

about 5000 K, is $\Delta T_{\rm eff} \approx 70$ K, $\Delta \log g \approx 0.3$ dex, $\Delta\xi_t \approx 0.5$ km s^{-1}.

The corresponding abundances shifts $\Delta \log \epsilon$ (X) caused by uncertainties in atmospheric parameters are tabulated in Table 2. Mainly, they do not exceed 0.15 dex. The main exception is an oxygen abundance determination error (as large as 0.16 dex) due to its sensitivity to temperature and gravity. Besides, the barium abundance, based on relatively strong lines, $\overline{W\,(\rm Ba)} = 140$ mÅ, could be disturbed by a large systematic error due to the sensitivity of its abundance to the microturbulent velocity value. We have to keep in mind, first, that the atmospheric parameters are not independent and such estimations of uncertainties are not absolutely valid and, second, that their influence on the relative abundances [X/Fe] is essentially reduced.

The dominant source of inaccuracy of chemical abundances is associated with inaccuracy of equivalent widths. Most of the lines used for computations of the chemical composition have equivalent widths W below 100 mÅ, resulting in very high demands on the quality of the observing material, since the accuracy of W values for weak lines, at a given spectral resolution, mainly depends upon the signal-to-noise ratio in the spectrum. The line–to–line scatter in the abundances σ (Table 3) is mainly contributed by uncertainities in measured equivalent widths W and in the gf–values. The scatter of element abundances derived from numerous ($n > 10$) lines is not so high, the rms deviation, σ, generally does not exceed 0.25 dex (cf. Table 3). It should be noted here that for elements having less than five lines the errors calculated are not a real estimation of an internal abundance scatter.

On the whole, we can expect abundances of elements with a sufficiently large number of lines (Si, Ca, Sc, Ti, Fe–peak) and gf–values of good quality, to be accurate within 0.20 to 0.25 dex and for other elements the uncertainty could be above 0.25–0.30 dex.

All computations in this study used the WIDTH9 code developed by Tsymbal (1996) for LTE. Corrections for hyperfine structure and for isotope shift causing broadening of Ni I, Mn I, and Ba II lines were not taken into account.

3. Discussion

3.1. The spectral features of K 413

The spectrum of K 413 exhibits several peculiar features, in particular, a complex absorption and emission profile of the Hα line (cf. Fig. 2). One can assume that the observed Hα profile is a superposition of the photospheric

Table 2. The uncertainties in the derived abundances $\Delta \log \epsilon\,(\mathrm{X})$ are due to errors in atmospheric parameters. The calculations were made using the model with $T_{\rm eff} = 4800\,\mathrm{K}$, $\log g = 0.7$, $\xi_{\rm t} = 3.5\,\mathrm{km\,s^{-1}}$.

	$\Delta \log \epsilon\,(\mathrm{X})$		
Species	$\Delta T_{\rm eff} = \pm 70\,\mathrm{K}$	$\Delta \log g = \pm 0.3\,\mathrm{dex}$	$\Delta \xi_{\rm t} = \pm 0.5\,\mathrm{km\,s^{-1}}$
C I	0.11	0.15	0.01
O I	0.16	0.16	0.02
Na I	0.04	0.03	0.03
Mg I	0.05	0.03	0.13
Al I	0.02	0.02	0.02
Si I	0.02	0.01	0.02
Si II	0.13	0.17	0.03
S I	0.09	0.13	0.01
Ca I	0.06	0.04	0.12
Sc II	0.01	0.13	0.07
Ti I	0.10	0.05	0.04
Ti II	0.03	0.11	0.12
V I	0.09	0.05	0.00
V II	0.04	0.12	0.00
Cr I	0.08	0.05	0.07
Cr II	0.07	0.12	0.01
Mn I	0.09	0.05	0.02
Fe I	0.07	0.04	0.09
Fe II	0.04	0.13	0.05
Ni I	0.08	0.03	0.04
Cu I	0.09	0.03	0.02
Zn I	0.05	0.04	0.08
Y II	0.01	0.11	0.04
Zr I	0.12	0.06	0.00
Zr II	0.01	0.12	0.01
Ba II	0.02	0.12	0.30
La II	0.01	0.12	0.00
Ce II	0.01	0.11	0.01
Nd II	0.02	0.12	0.01
Pr II	0.01	0.10	0.00
Eu II	0.00	0.12	0.01

absorption and the line formed in higher layers. Figure 2 shows the profiles of the Hα line for two observing moments in comparison with a photospheric (theoretical) profile. Such profiles were first found in the spectra of four globular cluster stars by Cohen (1976) using photographic echelle spectra recorded with a two-stage image tube. Then Mallia & Pagel (1978) raised the number of Hα-emission stars to 12 with the RGO spectrograph and a photon counter.

Recording spectra with a diode array at a three times poorer resolution compared to our resolution, Cacciari & Freeman (1983) surveyed spectra of bright stars in 12 globular clusters. One third of the stars with luminosities higher than solar by three orders of magnitude showed indications of Hα emission. The effect does not correlate with metallicity of the corresponding cluster. It follows from data in Table 3 of the cited paper that the velocity difference between the absorption core and the emission peaks does not significantly change from star to star, being about $50\,\mathrm{km\,s^{-1}}$. The mass loss rate was determined in the model of stellar wind, like in the studies by Cohen (1976) and by Mallia & Pagel (1978). Our Table 1 shows that the velocity difference between the core and the emission peaks for K 413 is in agreement with the general pattern of the Cacciari & Freeman (1983) survey.

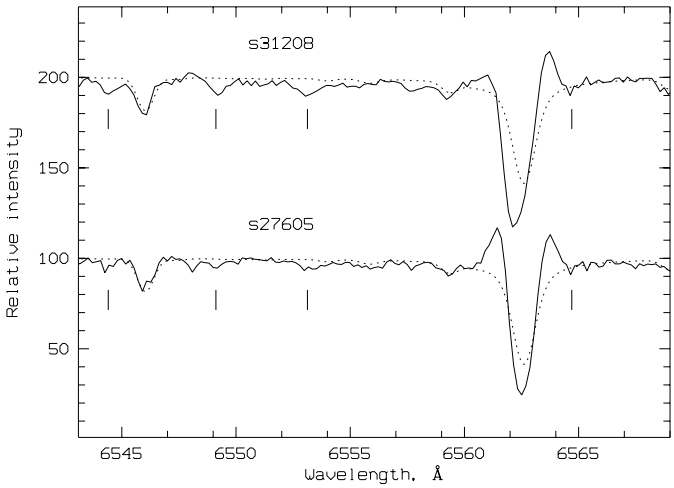

Fig. 2. Same as in Fig. 1 but for the wavelength region near the Hα line for two observing dates. The vertical ticks mark the telluric details.

Under the assumption of emission formed in an extended circumstellar envelope, the observed emission profiles can be obtained both for accretion on the star and for loss of matter. Indications of neither interstellar hydrogen (Knapp et al. 1973) nor dust (the results of the IRAS survey analyzed by Knapp et al. 1995) were found in globular clusters, thus the hypothesis of wind outflow of matter, with subsequent loss of this matter from the cluster as a whole, seems natural. The difference between the Hα emission of K 413 and the classical P Cygni profile can be due to a thinner circumstellar envelope and a lower mass loss rate. Low optical thickness follows also from the fact that no contribution from the envelope is observed for other strong lines of the photospheric spectrum (with the exception of the sodium resonance doublet). Mass loss rate estimates from Cacciari & Freeman (1983), Cohen (1976), Mallia & Pagel (1978) were essential for the problem of consistency of evolutionary computations of the RGB, HB, and AGB stages. It was noticed already in the first observations that the intensity ratio of the short-wave and long-wave residuals of the emission component differed from star to star and varied in time for each star. In the circumstellar envelope model, this means matter infall as well as outflow. However, the short time scale of such variations (several days) caused doubt on the hypothesis of an extended circumstellar envelope.

Other authors preferred the hypothesis that the Hα emission was formed in the lower chromosphere of cool luminous stars. Formation of the chromospheric absorption Hα component is photoionization-controlled; this conclusion, first formulated for the Sun, was long ago extended to most types of cool stars. An exception is represented by dMe dwarfs where photoionization corrections to the source function are low compared to impact corrections (Cram & Mullan 1979). Consequently, for most types of cool stars, the source function is insensitive to the structure of the chromosphere and is determined only by effective temperature and gravity. Cram & Mullan (1985)

Table 3. The chemical composition of K 413, $\log\epsilon(\mathrm{X})$ (for $\log\epsilon(\mathrm{H}) = 12.0$). In the table, n is the number of lines used; σ is the abundance dispersion derived for the given number of lines. Metallicity [Fe/H] and model parameters ($T_{\rm eff}$, $\log g$, $\xi_{\rm t}$) are given below the name of the object. The element abundances in the solar photosphere are from Grevesse et al. (1996).

Sun			K 413				BD + 18°2890 [2]
			−1.38, 4800 K, 0.7, 3.5 km s^{-1}				−1.48, 4790 K, 1.3, 1.2 km s^{-1}
Species	log ϵ(X)	X	log ϵ(X)	n	σ	[X/Fe]	[X/Fe]
C	8.55	C I	8.35	9	0.44	+1.18 [1]	+1.10
O	8.87	O I	9.66	3	0.15	+2.17	+0.91
Na	6.33	Na I	5.39	5	0.38	+0.44	−0.14
Mg	7.58	Mg I	6.81	4	0.04	+0.61	+0.26
Al	6.47	Al I	6.26	2		+1.17	+0.07
Si	7.55	Si I	6.68	19	0.26	+0.51	+0.28
		Si II	6.72	1		+0.55	+0.33
S	7.21	S I	7.01	4	0.24	+1.18	
Ca	6.36	Ca I	5.22	21	0.18	+0.24	+0.30
Sc	3.17	Sc II	1.62	11	0.13	−0.17	−0.22
Ti	5.02	Ti I	3.74	27	0.27	+0.10	−0.02
		Ti II	3.73	15	0.16	+0.09	+0.15
V	4.00	V I	2.76	9	0.28	+0.14	−0.36
		V II	2.71	4	0.24	+0.09	+0.15
Cr	5.67	Cr I	4.28	15	0.24	−0.01	−0.24
		Cr II	4.29	7	0.17	0.00	−0.04
Mn	5.39	Mn I	4.02	5	0.37	+0.01	−0.13
Fe	7.50	Fe I	6.14	180	0.24	+0.02	+0.01
		Fe II	6.09	22	0.23	−0.03	−0.02
Ni	6.25	Ni I	4.80	26	0.18	−0.07	−0.12
Cu	4.21	Cu I	2.41	3	0.22	−0.42	−0.54
Zn	4.60	Zn I	3.36	4	0.17	+0.14	−0.01
Y	2.24	Y II	0.55	7	0.26	−0.31	−0.57
Zr	2.60	Zr I	1.51	3	0.37	+0.29	+0.02
		Zr II	1.39	3	0.26	+0.17	−0.26
Ba	2.13	Ba II	0.63	3	0.19	−0.12	+0.04
La	1.22	La II	−0.23	3	0.29	−0.07	+0.20
Ce	1.55	Ce II	0.22	5	0.20	+0.05	−0.22
Nd	1.50	Nd II	−0.09	9	0.26	−0.21	−0.11
Pr	0.71	Pr II	−0.46	2		+0.21	+0.17
Eu	0.51	Eu II	−0.39	3	0.19	+0.48	+0.05

[1] This element's abundance was determined with a high uncertainty;

[2] Data for BD + 18°2890 from Klochkova et al. (2001a).

pointed out that observed Hα equivalent widths in the spectra of cool stars ($T_{\rm eff} < 5000$ K) were considerably higher than theoretical photospheric ones, whereas addition of a simple model chromosphere (two segments, with a linear change of temperature in each of them) made it possible to eliminate the discrepancy. They concluded that each cool star possessed a chromosphere with a significant optical depth in Hα. They also confirmed the old idea of nonthermal broadening of absorption profiles by the velocity field in the chromosphere. For supergiants, the pattern is more complicated than the cited models: somewhere for $\log g < 1.5$, increasing outflow rate must cause the situation when the hydrostatic approximation is not valid for the formation region of the Hα core. Our observations confirm both conclusions: the central absorption width of the observed Hα profile significantly exceeds the theoretical photospheric value, and the "residual" absorption exhibits a displacement of the core towards shorter wavelengths. The "blue" displacement of the absorption core evidence outflow; more exactly, the most peripheral of the core-forming layers move outward with respect to the layers forming the absorption profile at half intensity. The excess intensity of the short-wavelength residual of the chromospheric emission peak over the long-wavelength

one can be interpreted either as infall of absorption-forming layers with respect to emission-forming layers or as expansion of these layers, with deceleration (relative to the emission region). Note that the non-thermal broadening in the emission-forming region exceeds that for the external chromosphere.

Dupree et al. (1984) demonstrated that Hα emission could be formed in dense, hot chromospheres. The high sensitivity of the profile to the chromospheric temperature permits us to conclude that the presence of emission wings is not direct proof of matter outflow. Conclusive evidence can be asymmetry of the central absorption or different intensities of residual emission peaks. Smith & Dupree (1988) studied spectra of 52 halo giants (echelle spectrograph with Reticon) and found emission wings of the Hα line for 10 stars with $M_V < -1\overset{\mathrm{m}}{.}7$. Profile widths, their variability and different ratios of the short-wave component to the long-wave can be explained by differential motions in the chromospheric region with relatively high density and $T = 7000$ K to 8000 K, where the emission is formed. Adding data on chromospheric components of the resonance Mg II and Ca II lines made it possible to finally conclude in favor of the chromospheric origin of the Hα emission (Dupree et al. 1990).

Besides progress in model description, the development of the chromospheric hypothesis is due to improvement of observational possibilities. With better spectroscopic resolution and signal-to-noise ratio, the fraction of luminous stars with revealed Hα emission increases: it was 30% in Cacciari & Freeman (1983), 60% in Gratton et al. (1984), 72% in Bates et al. (1993). The displacement of the Hα absorption core correlates with the star's luminosity and with the core displacements for the resonance sodium doublet lines (Kemp & Bates 1995). As it can be seen in Fig. 2, the Hα profile in the K 413 spectrum is time variable, which also confirms the chromospheric origin of its emission.

The second characteristic feature of the spectrum of K 413 is the presence of several absorptions we identify with diffuse interstellar bands (DIBs). The technique we use to isolate such bands is the same as in Klochkova et al. (2000). The equivalent widths of the most easily detectable bands, λ 6203, 6379, 6613 ÅÅ, are respectively W = 24, 20, and 66 mÅ. The best-known band, λ 5780 (Fig. 3), is blended with the star's lines and so it is impossible to measure its parameters separately. Thus, absorption bands, most probably formed in the stellar vicinity, have been revealed in the spectrum of an evolved star, a globular cluster member. Earlier, such spectral features were found for several evolved stars: Cohen & Jones (1987) discovered diffuse interstellar bands in the spectrum of the heavily reddened nucleus of the planetary nebula WC11; Le Bertre & Lequeux (1993) studied a sample of stars featuring mass loss and revealed diffuse interstellar bands in the spectra of IRC +10420 and AC Her. In the cause of the present program, we also found diffuse interstellar absorptions in the spectra of several cool post-AGB objects (cf. Klochkova 2000 and references therein).

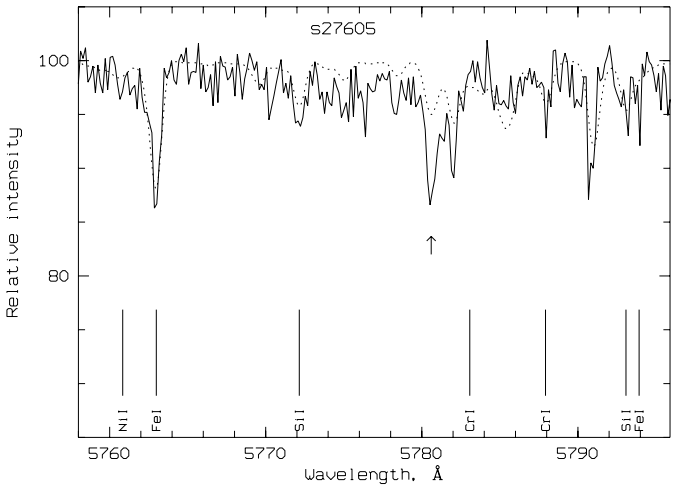

Fig. 3. Same as in Fig. 1 but for the wavelength region with the strongest DIB λ 5780 Å (marked with an arrow).

From the cluster membership of K 413, taking into account the mean color excess, $E(B-V) = 0.19$, and the distance modulus, $m - M = 14\overset{\mathrm{m}}{.}02$ (Harris 1996), we obtain the star's absolute magnitude, $M_v = -1\overset{\mathrm{m}}{.}8$. The real reddening value for K 413 can be much higher because of the additional circumstellar reddening revealing itself in the absorption bands (like the 5780 Å band in Fig. 3). In such a case, the star's luminosity can be considerably higher.

Revealing absorption bands in the spectrum of a globular-cluster star is an unexpected result: as stated above, searches for dust in the regions of globular clusters, making use of the IRAS data, gave negative results (Lynch & Rossano 1990).

3.2. The chemical composition

Until now, estimates of metallicity for the cluster M 12 were based only on photometric data or on low-resolution spectra. From observations of the Ca II triplet (8498, 8542, 8662 Å), Da Costa & Armandroff (1995) derived [Fe/H] = −1.34 and attributed M 12 to the intermediate subsystem of globular clusters. However, Rutledge et al. (1997), also from low-resolution intensities of the Ca II triplet, found a higher metal abundance, [Fe/H] = −1.14. Carretta & Gratton (1997), from high-resolution spectroscopic observations of several stars in selected globular clusters, suggested a new uniform metallicity scale for a large sample of globular clusters. For M 12, they obtained [Fe/H] = −1.37.

Chemical element abundances, $\log \epsilon(\mathrm{X}) \pm \delta$, averaged over the measured lines, are collected in Table 3. Its second column reproduces, from Grevesse et al. (1996), the corresponding data for the solar atmosphere we use to determine the relative abundances,

$$[\mathrm{X/Fe}] = [\log \epsilon(\mathrm{X}) - \log \epsilon(\mathrm{Fe})]_* - [\log \epsilon(\mathrm{X}) - \log \epsilon(\mathrm{Fe})]_\odot,$$

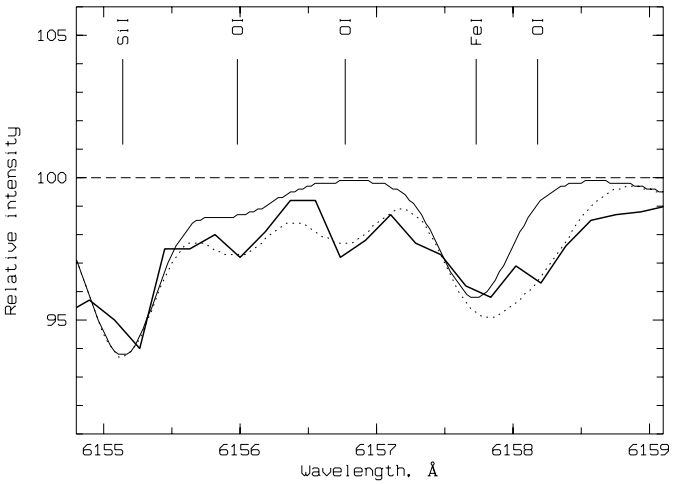

Fig. 4. Same as in Fig. 1 but for the wavelength region of the spectrum of K 413 containing O I oxygen lines near 6156 Å. The dashed line shows the position of the continuum. The thin line shows the theoretical spectrum calculated with the model parameters and chemical compostion from the table, but the value [O/Fe] = 0.

needed to analyze the element abundance curve. Below we discuss the abundance distribution in the atmosphere of the studied star in more detail.

For comparison, Table 3 presents the chemical composition of BD + 18°2890, a luminous star at a high galactic latitude. Klochkova et al. (2001a), from a variety of its characteristics, concluded that the high-latitude supergiant BD + 18°2890, having [Fe/H] = −1.48, probably belonged to the early post-AGB evolution stage.

The metallicity value derived by us for K 413, [Fe/H] = −1.38, is in a good agreement with the results of Carretta & Gratton (1997). The mean abundance of the iron-peak metals (vanadium, chromium, manganese, nickel) does not differ considerably from that of iron: for K 413, [Met/Fe] = 0.01. Copper, being an iron-peak element not universally recognized (Timmes et al. 1995), shows a slight deficiency, [Cu/Fe] = −0.42; this value has been reliably established from 3 lines. Sneden et al. (1991) concluded that similar copper underabundance was observed for halo stars in globular clusters as well as in the galactic field.

The most interesting feature in the distribution of abundances for K 413 is the large oxygen excess ([O/Fe] = +2.17) revealed from 3 confidently measured O I lines around 6156 Å (see Table 4). Unfortunately, the lines of the IR oxygen triplet λ 7773 Å in the available spectrum of K 413 are at the very edge of the echelle frame, so we did not apply these lines either for oxygen abundance or luminosity determinations. To illustrate the determination of [O/Fe] ratio, we present Fig. 4 showing a comparison between the observed spectrum and the theoretical one calculated for two values [O/Fe] = +2.2 and [O/Fe] = +0.0 computed with the STARSP code (Tsymbal 1996). This oxygen overabundance, [O/Fe] = +2.17, is much higher than the value observed in the atmospheres of

Table 4. Atomic data (lower-level excitation potentials EP, oscillator strengths gf, equivalent widths W) of O I lines and corresponding abundances ϵ(O).

λ Å	EP, eV	lg gf	W	ϵ(X)
O I				
6155.98	10.74	−0.66	12	9.83
6156.77	10.74	−0.44	11	9.56
6158.18	10.74	−0.29	15	9.60
7771.94	9.15	0.33	105	9.01
7775.39	9.15	−0.03	99	9.30

halo unevolved stars (Timmes et al. 1995), so we conclude the presence of dredge-up of oxygen produced in helium burning.

The carbon abundance, [C/Fe] = +1.18, has been determined from nine C I lines in the spectrum of K 413. This value has a large uncertainty because of low intensity of the C I lines. Besides, the most reliable lines around 7110 Å are blended with telluric lines. The nitrogen lines, N I 7423, 7442, 7468 ÅÅ, are strong enough, but since the wavelength region with these lines was recorded at the edge of our echelle frame, where line positions could be measured with poor accuracy, we do not present the nitrogen abundance because of its low reliability.

From four lines, we derive a normal zinc abundance, relative to iron, for K 413: [Zn/Fe] = +0.14. Just the abundance of zinc, not changing in the course of the stellar nucleosynthesis in the interiors of low- and intermediate-mass stars, varies over a wide metallicity range by the same amount as the iron abundance (Sneden et al. 1991). Thus the conclusion on zinc abundance is independent of the scale used (a relative or absolute one). This fact, together with the practically normal value, [Zn/Fe] = +0.14, leads to the conclusion of no selective separation of chemical elements in the probable circumstellar envelope of K 413. This conclusion is also supported by the good agreement between the metallicity of K 413 and that for the cluster as a whole.

Now consider the abundances of light metals in the atmosphere of K 413. From the group of odd α-process elements, we have obtained data for sodium and aluminum. Sodium is slightly enhanced, [Na/Fe] = +0.44; Denissenkov & Ivanov (1987) and Denissenkov (1989) showed that such an excess could be due to synthesis of sodium in the process of hydrogen burning. However, the obtained sodium excess is probably due, in part, to no treatment of deviations from the local thermodynamic equilibrium (LTE). Mashonkina et al. (2000) demonstrated that, for a luminous star with $T_{\rm eff} \approx 5000$ K, accounting for superionization of sodium atoms leads to corrections of about −0.2 dex to sodium abundance, compared to the LTE approximation, for the subordinate sodium lines used by us. Consequently, a considerable part of the sodium excess revealed by us is probably of methodological, not evolutionary, origin.

The high abundance of aluminum derived by us from two lines is not a rare case for stars in globular clusters with moderate metal deficiency, as it follows from Shetrone (1996). However, K 413 is peculiar in the way that its aluminum excess is accompanied by oxygen excess, whereas, according to Shetrone (1996), an Al–O anticorrelation is observed for globular cluster giants. We explain this anomaly of the chemical composition of K 413 by its more advanced evolutionary stage.

Of even α-process elements, we determined abundances for Mg, Si, S, Ca, and Ti. Note that titanium (like scandium) is an intermediate element, sometimes considered the heaviest α-process element and sometimes, the lightest iron-peak metal (Wheeler et al. 1989). In the case of K 413, the abundances of Sc and Ti correspond to that of iron.

The excess silicon abundance, [Si/Fe] = +0.53, has been reliably determined from two ionization states. Similar relative silicon abundances, [Si/Fe], are also observed in the atmospheres of unevolved stars with metallicities close to that of K 413 (Timmes et al. 1995). Consequently, from our data, we can conclude a normal silicon abundance for K 413. However, the silicon excess in the atmosphere of BD + 18°2890, a luminous star in the galactic field (Table 3), is somewhat lower.

Klochkova et al. (2001a) have already noted that sulphur abundances in the atmospheres of evolved stars seem to be a special problem. Earlier, Bond & Luck (1987) revealed a large sulphur excess, [S/Fe] = +1.2, in the atmosphere of the low-metallicity post-AGB star HD 46703 and explained it with probable synthesis of sulphur by addition of α particles to C^{12} nuclei. However, Klochkova (1995) found an excess abundance of sulphur in the atmosphere of the normal massive supergiant α Per. First, it has no circumstellar envelope and thus there are no condensation processes; second, we cannot expect any manifestations of synthesis of sulphur at such an early evolutionary stage. Sulphur excess seems to be a persistent feature in the pattern of the chemical composition of evolved stars (besides the results in Bond & Luck 1987, cf., for instance, Klochkova 1995; Van Winckel et al. 1996; Klochkova et al. 1999, 2000). For these reasons, we still rather tend to explain the observed excess of sulphur in the atmosphere of K 413 by methodotogical reasons.

It should be noted that the abundance of sulphur, relative to iron, is also enhanced in the atmospheres of unevolved stars (Timmes et al. 1995 and references therein). Recently were published also new results concerning sulphur abundances. Using the near-infrared S I doublet, Israelian & Rebolo (2001) derived enhanced sulphur abundances for some unevolved metal-poor stars. These authors concluded that an the increasing of [S/Fe] ratio for most metal-deficient stars could be explained through the increasing role of of hypernovae in the earliest evolution of the Galaxy.

A very important characteristic of the chemical composition of evolved stars is the abundance of heavy elements, formed in the synthesis due to the slow process of neutron capture. It is usually accepted (Schwarzschild & Härm 1965; Lattanzio & Forestini 1999; Blöcker 2001) that an excess of heavy metals can be observed in the atmospheres of post-AGB stars, due to neutron capture, mixing, and dredge-up of matter processed in the interiors to the surface. The data in Table 3 rather show depleted abundances of these elements in the atmosphere of K 413. In particular, the abundance of barium, confidently determined from three lines, is [Ba/Fe] = −0.12, in agreement with the general trend of this ratio for halo stars (McWilliam 1997). The relative abundances of lighter s-process metals, Y and Zr, have been determined less accurately because of the limited number of lines available, but on average in this case, too, their relative abundance, $[s/\mathrm{Fe}] = -0.04$, appears to be close to the solar value.

We noted earlier (Klochkova et al. 2001b) that deficiency of s-process elements in the atmospheres of supergiants, also at the post-AGB stage, was observed much more often than their excess. Both physical and methodical reasons for the deficiency were frequently discussed (see, for example, Luck & Bond 1989). In our opinion, the lack of heavy elements' dredge-up manifestations observed for most supergiants is real and not due to systematic errors of model atmosphere analysis for spectra of supergiants. Most probably, presence or absence of excess for s-process elements is somehow related to such fundamental parameters of the star as its initial mass and mass loss rate, determining the evolution of an individual star.

As for heavier elements, with $Z \geq 57$ (La, Ce, Nd, Pr), we can generally speak about complete agreement with the solar relative abundance of these elements: [heavy/Fe] = 0.0. Such a pattern agrees with a behaviour of lanthanides in halo and in globular cluster stars (Travaglio et al. 1999; Wheeler et al. 1989). At the moderate metal deficiency, these elements represent products of both slow and rapid neutron captures.

A slight excess of europium (created only in the r-process), [Eu/Fe] = +0.48, is typical of stars in low-metallicity globular clusters (Shetrone 1996). The value log (Ba/Eu) is a traditional contribution indicator for r- and s-processes for the synthesis of these metals. The value log(Ba/Eu) ≈ 1 for K 413 is in agreement with the general pattern for the halo (Spite 1992; Timmes et al. 1995).

Comparing the data in Table 3, we can conclude that the main parameters and details of the chemical composition of K 413 are close to the corresponding parameters for BD + 18°2890. Taken together, the features of the chemical composition (excess of oxygen and of α-process elements), combined with the star's position in the color-magnitude diagram, make us assume the post-AGB evolutionary stage for K 413.

Such post-AGB objects are frequently met in globular clusters. For example, Huges and Wallerstein (1997) attributed the star N 13 (with the absolute magnitude $M_V = -2.06$) in the cluster M 15 to this stage of evolution. It appears from the color-magnitude diagram (Brocato et al. 1996) that M 12 has other stars with $V < 13$ and $(B - V) < 1$.

From the main peculiarities of its chemical composition (excess of O, excess of light metals: Na, Mg, Al; no excess of *s*-process elements), K 413 is a hotter analog of the "CO-normal" group of stars, Nos. 74, 91, and 256 in the cluster ω Cen, the latter's chemical composition studied by Francois et al. (1988). Note, however, that, for the stars 74, 91, and 256, the relative abundances of the *s*-process elements, [heavy/Fe], are depleted by the factor of 3 to 4 compared to the solar value, whereas for K 413, the value of [heavy/Fe] is closer to that for the Sun. By the presence of emission in the wings of the Hα line, K 413 is similar to the star 65 in ω Cen.

At the same time, the chemical composition of K 413 differs drastically from that of the highly evolved star ROA 24 (Ferenbach's star) in the cluster ω Cen. Gonzalez & Wallerstein (1992) determined the detailed chemical composition of ROA 24 from high-resolution spectra. The large excesses of CNO elements and *s*-process metals in its atmosphere, along with its high luminosity, evidence for the AGB (or post-AGB) evolutionary stage. It should be noted that the significantly different effective temperatures of K 413 and ROA 24 cannot be a key issue for explanation of the principal differences between the chemical compositions of the two stars. The cluster ω Cen contains a sample of luminous stars with effective temperatures around 4100–4500 K, both with barium excesses and barium deficiencies (cf. Fig. 3 in Gonzalez & Wallerstein 1992). Later, Gonzalez & Wallerstein (1994) came to the conclusion that the main parameter determining the dredge-up of the synthesis products to a star's atmosphere at the post-AGB stage was its luminosity. Their conclusion is confirmed by the fact that ROA 24 is the most luminous star in the Galaxy's system of globular clusters.

3.3. Radial velocities

Detailed information of the velocity pattern in the atmosphere is needed to clarify the object's evolutionary status. The results of our radial velocity measurements for K 413 are presented in Table 1. To improve accuracy of velocity determinations, we compared the observed spectrum with the corresponding synthetic one and selected unblended lines. The positional zero point for each spectrogram was determined in the standard way, relative to ionospheric emissions of the night sky and to the absorption telluric spectrum, recorded with the object's spectrum.

The typical uncertainty of the average was $\delta = 0.2\,\mathrm{km\,s^{-1}}$, for the number of lines exceeding 400 and the measurement uncertainty for a single line $\sigma \approx 3.4\,\mathrm{km\,s^{-1}}$. The mean velocity from lines of metals, $\mathrm{V_r(met)} = -40.96\,\mathrm{km\,s^{-1}}$ for the spectrum s27605 and $-41.48\,\mathrm{km\,s^{-1}}$ for the second one, can be considered the systemic velocity; it is in good agreement with the radial velocity value, $V_\mathrm{r} = -41.3\,\mathrm{km\,s^{-1}}$, found by Harris et al. (1983) for the whole cluster from low-resolution spectra. The agreement between radial velocities of K 413 obtained in this study and by Harris et al. (1983) more than 20 years earlier permits us to conclude that the star's radial velocity is constant. Thus, we can reject the suspicion of possible binarity of K 413, the star occupying a peculiar position in the color-magnitude diagram.

As noted above, the Hα line has a complex emission and absorption profile with two emission peaks, at the velocities $V_\mathrm{em,blue} = -88.2$ and $V_\mathrm{em,red} = +17.4\,\mathrm{km\,s^{-1}}$ for the spectrum s27605, differing from the systemic velocity correspondingly by -47.2 and $+58.3\,\mathrm{km\,s^{-1}}$.

It follows from the data in Table 1 that the absorption core of the Hα line has a velocity differing from the mean metallic-line radial velocity of the star by more than one rms error. This displacement of the absorption component towards shorter wavelengths is also clearly seen in Fig. 2, where the position of the core of the theoretical Hα profile corresponds to the star's velocity derived from the absorption lines of metals.

The mean radial velocity values measured from several diffuse bands we identified in the spectrum of K 413 are collected in Table 1. It is natural to assume that these absorptions are formed in the circumstellar region: their interstellar origin is improbable because of the cluster's high position in the Galaxy ($b = 26.^\circ3$). The difference between the radial velocities measured in the spectrum of K 413 from lines formed in the photosphere and from those formed in the circumstellar envelope gives a negative value for the velocity of the envelope's motion with respect to the central star, $\Delta V_\mathrm{r} = -16.8\,\mathrm{km\,s^{-1}}$, and thus we have reason to consider infall of the circumstellar matter onto the star.

It was already noted above that, according to Smith & Dupree (1988), the excess intensity of the short-wavelength emission component of the Hα line over the long-wavelength one (such an intensity ratio of the emission peaks is characteristic of K 413) is evidence is for decelerating matter outflow in the star's chromosphere. But we see the opposite behavior in two Hα profiles obtained for two observing moments.

The lines of the resonance sodium doublet, Na D1, 2, are asymmetric in the spectrum of K 413, their cores shifted to longer wavelengths. Measurements show that both lines are blends, poorly resolved at our spectral resolution, and each of them consists of two components (see Table 1). One of the components has the velocity coinciding with that of the star, and the position of the second component corresponds to the velocity measured from diffuse bands. Peterson (1981) was the first to notice asymmetry of the sodium doublet lines in the spectra of globular-cluster giants. A detailed study of displacements of the sodium doublet lines with respect to stellar velocities, based upon high-resolution spectra, was performed by Bates et al. (1993) for the clusters M 22 and ω Cen. For a sample of program stars, these authors revealed displacements of the doublet lines approximately within the -10 to $+2\,\mathrm{km\,s^{-1}}$ range, interpreted as a manifestation of matter outflow (or infall, in the cases of positive displacements) in stellar envelopes. In particular, analyzing their data, Bates et al. (1993) concluded that

displacements of the Na doublet lines were observed for luminous stars, $L_{\odot} \approx 3.0$. This result can be considered additional evidence in favor of our assumption of the higher luminosity of K 413 compared to the value derived from its cluster membership.

4. Conclusions

From CCD spectra obtained with the echelle spectrometer of the 6 m telescope, using model atmospheres, we determined the fundamental parameters $T_{\rm eff} = 4800\,{\rm K}$, $\log g = 0.7$ and the detailed chemical composition for the star K 413 in the globular cluster M 12. The measured radial velocity of the star for two observing moments $V_{\rm r} = -40.96$ and $-41.48\,{\rm km\,s^{-1}}$, agrees very well with the mean velocity of M 12, confirming cluster membership of the star.

The most important feature in the optical spectrum of K 413 is the presence of emission components in the wings of the Hα line, with two variable emission peaks.

The spectrum of K 413 contains absorption bands, with positions making it possible to identify them with the so-called diffuse interstellar bands. The difference between the radial velocity corresponding to these bands and the star's velocity is $\Delta V_{\rm r} = 16.8\,{\rm km\,s^{-1}}$. The sodium doublet lines, Na D1, 2, are blends, with one of their components having the same displacement towards longer wavelengths.

The obtained value [Fe/H] $= -1.38$ is the first determination of metallicity for the cluster M 12 from high-resolution spectra. This metallicity value agrees well with the published mean metallicity of M 12, derived from photometry and low-resolution spectroscopy.

The principal anomaly of the chemical composition of the star's atmosphere is a large oxygen excess, [O/Fe] $\approx +2.2$.

The *s*-process metals are depleted relative to metallicity: for Y and Zr, [X/Fe] $= -0.04$, and for barium, [Ba/Fe] $= -0.12$. The abundances of heavier elements: La, Ce, Nd, and Pr, do not differ from solar with respect to iron: [X/Fe] $= 0.0$. The europium excess, [Eu/Fe] $= +0.48$, is characteristic of stars in low-metallicity globular clusters.

The star's position in the color-magnitude diagram of the cluster M 12 and its chemical composition permit us to suppose that K 413 is in the post-AGB stage of evolution.

Acknowledgements. The authors are grateful to N. S. Tavolganskaya for her great help in spectral reductions.

We are much indebted to our referee for critical reading of the manuscript and for his valuable notes and comments.

One of the authors (V.G.K.) wishes to thank the Russian Foundation for Basic Research for financial support of the spectroscopic investigations, with the 6–meter telescope, of objects evolving from AGB stars to planetary nebulae (project 99-02-18339) and the Federal "Astronomy" Program (project 1.4.1.1.). The research described in this publication was made possible in part by Award No. RP1–2264 of the the U.S. Civil Research & Development Foundation for the Independent States of the Former Soviet Union (CRDF).

N.N.S. would like to thank the council of the program of support for Russia's leading scientific schools, for financial support (grant 00-15-96627).

This study made use of the SIMBAD astronomical data base, of the CDS bibliographic data base, and of the VALD atomic data base.

References

Bates, B., Kemp, S. N., & Montgomery, A. S. 1993, A&AS, 97, 937
Blöcker, T. 2001, Astrophys. Space Sci., 275, 1
Bond, H. E., & Luck, R. E. 1987, ApJ, 312, 203
Brocato, E., Buonanno, R., Malakhova, Y., & Piersimoni, A. M. 1996, A&A, 311, 778
Cacciari, C., & Freeman K. C. 1983, ApJ, 268, 185
Carretta, E., & Gratton, R. G. 1997, A&AS, 121, 95
Cohen, J. G. 1976, ApJ, 203, 127
Cohen, M., & Jones, B. F. 1987, ApJ, 321, L151
Da Costa, G. S., & Armandroff, T. E. 1995, AJ, 109, 2533
Cram, L. E., & Mullan, D. J. 1979, ApJ, 234, 579
Cram, L. E., & Mullan, D. J. 1985, ApJ, 294, 626
Denissenkov, P. A., & Ivanov, V. V. 1987, Astro. Lett., 13, 520
Denissenkov, P. A. 1989, Astro. Lett., 14, 1023
Dupree, A. K., Hartmann, L., & Avrett, E. H. 1984, ApJ, 281, L37
Dupree, A. K., Harper, G. M., Hartmann, L., et al. 1990, ApJ, 361, L9
Francois, P., Spite, M., & Spite, F. 1988, A&A, 191, 267
Galazutdinov, G. A. 1992, Preprint Spec. Astrophys. Observ., No. 92
Geffert, M., Tucholke, H.-J., Georgiev, Ts. B., & Le Campion, J.-F. 1991, A&AS, 91, 487
Gonzalez, G., & Wallerstein G. 1992, MNRAS, 254, 343
Gonzalez, G., & Wallerstein, G. 1994, AJ, 108, 1325
Gratton, R. G., Pilachowski, C. A., & Sneden, C. 1984, A&A, 132, 11
Grevesse, N., Noels, A., & Sauval, A. J. 1996, ASP Conf. Ser., 99, 117
Gustafsson, B., Bell, R. A., Eriksson, K., & Nordlund, Å. 1975, A&A, 42, 407
Harris, W. E. 1996, AJ, 112, 1487
Harris, H. C., Nemec, J. M., & Hesser, J. E. 1983, PASP, 95, 256
Huges, J., & Wallerstein, G. 1997, PASP, 109, 274
Israelian, G., & Rebolo, R. 2001, arXiv [astro-ph/0107072 4Jul2001]
Kemp, S. N., & Bates, B. 1995, A&AS, 112, 513
Klochkova, V. G. 1995, MNRAS, 272, 710
Klochkova, V. G., & Galazutdinov, G. A. 1991, Preprint Spec. Astrophys. Observ., No. 71
Klochkova, V. G., Szczerba, R., Panchuk, V. E., & Volk, K. 1999, A&A, 345, 905
Klochkova, V. G., Szczerba, R., & Panchuk, V. E. 2000, Astro. Lett., 26, 510
Klochkova, V. G., Zhao, G., Panchuk, V. E., & Tavolganskaya, N. S. 2001a, Astron. Rep., 45(7), 553
Klochkova, V. G., Panchuk, V. E., & Tavolganskaya, N. S 2001b, Astro. Lett., accepted
Knapp, G. R., Rose, W. K., & Kerr, F. J. 1973, ApJ, 186, 831
Knapp, G. R., Gunn, J. E., & Connolly, A. J. 1995, ApJ, 448, 195
Küstner, F. 1933, Veröff., Astron. Inst. Bonn., 26, 1

Lattanzio, J., & Forestini, M. 1999, in Asymptotic giant branch stars, Proceed, IAU Symp. 191, ed. T., Le Bertre, A., Lébre, & C. Waelkens, PASP, 31
Le Bertre, T., & Lequeux, J. 1993, A&A, 274, 909
Luck, R. E., & Bond, H. E. 1989, ApJ, 342, 476
Lynch, D. K., & Rossano, G. S. 1990, AJ, 100, 719
Mallia, E. A., & Pagel, B. E. J. 1978, MNRAS, 184, 55
Mashonkina, L. I., Shimansky, V. V., & Sakhibullin, N. A. 2000, AZh, 77, 893
McWilliam, A. 1997, ARA&A, 35, 503
Panchuk, V. E., Najdenov, I. D., Klochkova, V. G., et al. 1998, Bull. Spec. Astrophys. Observ., 44, 127
Peterson, R. C. 1981, ApJ, 248, L31
Racine, R. 1971, AJ, 76, 331
Rutledge, G. A., Hesser, J. E., Stetson, P. B., et al. 1997, PASP, 109, 883
Schwarzshild, M., & Härm, R. 1965, ApJ, 142, 855
Shetrone, M. D. 1996, AJ, 112, 1517
Smith, G. H., & Dupree, A. K. 1988, AJ, 95, 1547
Sneden, C., Gratton, R. G., & Crocker, D. A. 1991, A&A, 246, 354
Spite, M. 1992, in The stellar populations of Galaxies, IAU Symp. 149, ed. B. Barbuy, & A. Renzini (The Netherlands), 123
Timmes, F. X., Woosley, S. E., & Weaver, T. A. 1995, ApJS, 98, 617
Travaglio, C., Galli, D., Gallino, R., et al. 1999, ApJ, 521, 691
Tsymbal, V. 1996, in Model Atmospheres and Spectrum Synthesis, ed. S. J. Adelman, F. Kupka, & W. W. Weiss, ASP Conf. Ser., 108, 198
Wheeler, J. C., Sneden, C., & Truran, J. W. 1989, ARA&A, 27, 279
Van Winckel, H., Waelkens, C., & Waters, L. B. F. M. 1996, A&A, 306, L37
Zinn, R. J., Newel, E. B., & Gibson, J. B. 1972, A&A, 18, 390